NSRRC-J05276 (2016)

www.nature.com/scientificreports

SCIENTIFIC REPORTS

OPEN

Revisit the Correlation between the Elastic Mechanics and Fusion of Lipid Membranes

Received: 28 April 2016
Accepted: 18 July 2016
Published: 18 August 2016

Zih-An Fan*, Kuan-Yu Tsang*, Si-Han Chen & Yi-Fan Chen

Membrane fusion is a vital process in key cellular events. The fusion capability of a membrane depends on its elastic properties and varies with its lipid composition. It is believed that as the composition varies, the consequent change in C_0 (monolayer spontaneous curvature) is the major factor dictating fusion, owing to the associated variation in G_Es (elastic energies) of the fusion intermediates (e.g. stalk). By exploring the correlations among fusion, C_0 and K_{cp} (monolayer bending modulus), we revisit this long-held belief and re-examine the fusogenic contributions of some relevant factors. We observe that not only C_0 but also K_{cp} variations affect fusion, with depression in K_{cp} leading to suppression in fusion. Variations in G_Es and inter-membrane interactions cannot account for the K_{cp}-fusion correlation; fusion is suppressed even as the G_Es decrease with K_{cp}, indicating the presence of factor(s) with fusogenic importance overtaking that of G_E. Furthermore, analyses find that the C_0 influence on fusion is effected via modulating G_E of the pre-fusion planar membrane, rather than stalk. The results support a recent proposition calling for a paradigm shift from the conventional view of fusion and may reshape our understanding to the roles of fusogenic proteins in regulating cellular fusion machineries.

Membrane fusion is vital for living organisms. Many cellular events, such as the release of neurotransmitters, the invasion of enveloped viruses, the intracellular trafficking of proteins and the conception for sexual reproduction, involve membrane fusion[1,2]. Complete of the fusion process sees two membrane-bound entities merge into a single one, with the initially discrete membranes and the enclosed contents mixed together. Cellular implementation of fusion requires the concerted action of an intricate machinery consisting of lipids, fusogenic proteins and fusion-triggering stimulants (*e.g.*, Ca^{2+})[3,4]. While the wide diversity of the lipids, proteins and other biomolecules involved in cellular fusion often complicates the attempts to explore the inner working shared by various fusion machineries, protein-free model membranes with defined lipid compositions [*e.g.*, liposome, also known as unilamellar vesicle (ULV), a hollow spherical structure bound with a *single* lipid bilayer] have been proven an indispensable tool in uncovering the universal mechanism for all sorts of fusion[3,5].

It is known from model membrane studies that initiating and advancing the fusion process demand the overcoming of several energy barriers; recognizing these barriers has provided insight on how proteins regulate cellular fusion machineries[3,5]. The first energy barrier arises from the need to bring two fusion-destined membranes into close proximity to initiate fusion[6,7]. The barrier, an inter-membrane interaction known as hydration repulsion, results from the resistance to removing inter-membrane water needed for shortening the inter-membrane distance[8]. Once fusion is initiated, the next energy barriers are related to the structural transformations of the *cis*-monolayers (the proximal leaflets of the lipid bilayers undergoing fusion)[4,9]. Theoretical studies predict that the monolayers transform from the initial planar conformation to two fusion intermediate structures, hemifusion stalk and hemifusion diaphragm (HD), before forming a fusion pore (FP) to complete the process. The hemifusion structures are highly curved. Analogous to the well-studied lamellar ↔ nonlamellar phase transitions of lipid dispersions[10], the transition from planar monolayers to the hemifusion structures also entails the membrane deformations that implicate the *monolayer* elastic energy density, g_E,

$$g_E = \frac{1}{2}K_{cp}(C - C_0)^2 + K_G G \quad (1)$$

Department of Chemical and Materials Engineering, National Central University, No. 300, Zhongda Rd., Zhongli District, Taoyuan 32001, Taiwan. *These authors contributed equally to this work. Correspondence and requests for materials should be addressed to Y.-F.C. (email: yifanchen@ncu.edu.tw)

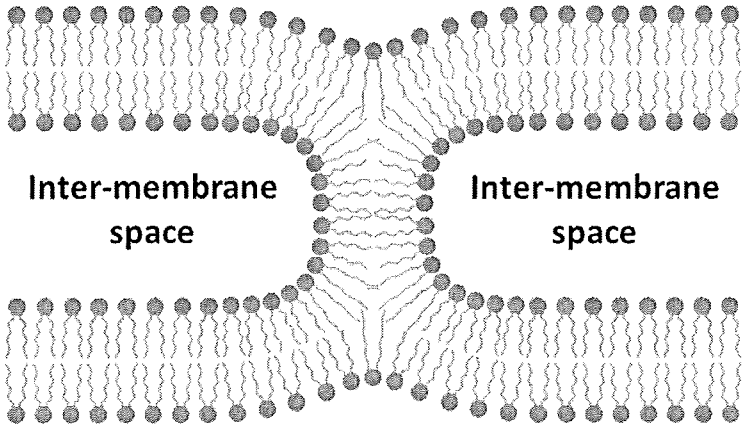

Figure 1. Hemifusion stalk. Color encodes the origins of the lipid molecules. In this fusion stage, the lipid molecules of the two *cis*-monolayers have intermixed while the *trans*-monolayers and the contents are still separated.

where K_{cp} is the monolayer bending modulus, C the total curvature, C_0 the monolayer spontaneous curvature (the molar-weighted average of the C_0s of the constituting lipids), K_G the Gaussian modulus and G the Gaussian curvature[11,12]. When free of any external constraint, a monolayer of a specific C_0 tends to form a structure with $C = C_0$. Any deviation of C from C_0 increases g_E, destabilizes the monolayer structure possessing the given C and raises the energy barrier to the formation of this structure. Accordingly, a monolayer having $|C_0| >> 0$ exhibits a high tendency of forming nonlamellar structures, with the sign of the C_0 indicating its preference for normal (positive) or inverted (negative) nonlamellar structures, while monolayers with $|C_0| \approx 0$ prefer a planar conformation.

The energy barriers, and thus the fusion capability, can be reduced/raised by tuning the membrane composition. Experiments show that adjusting the composition of a ULV alters its fusion capability considerably, which is attributable to the consequent changes in g_E and/or hydration repulsion[6,13]. Conventionally, the former is considered as the major factor affecting fusion and is induced by introducing to membranes the lipids of negative C_0s, because hemifusion stalk, whose existence has been experimentally confirmed[14], is a structure with negative Cs for the *cis*-monolayers (Fig. 1). Nevertheless, varying C_0 is merely one approach to change g_E; varying K_{cp} can be another, as manifested in Equation (1). While many efforts have been dedicated to exploring the effects of varying C_0 on fusion and their underlying mechanisms, few, if any, take on the issue of how, or even whether, the change in K_{cp} affects the energy barriers and thus fusion of a membrane, even though such investigations will surely provide further insight. Moreover, a recent X-ray study demonstrated the need to shift the conventional "C_0-centered" view on fusion because hydration repulsion was proven as energetically important as g_E, if not more so, to fusion[6]. It is therefore of great value to re-examine the fusogenic importance of elastic mechanics and explore the fusogenic relevance of other factors.

This study aspires to address these issues and provide further insight on the fusion mechanisms of protein-free lipid membranes, in the hope that the learned knowledge will advance our understanding to the working principles general to fusogenic proteins. Several experimental techniques (*e.g.*, X-ray diffraction, the electron density reconstruction and fluorescence spectroscopy) have been employed and an experimental scheme (specifically for the K_{cp} measurements) developed to measure 1) the C_0s and K_{cp}s of several lipid species [*i.e.*, the species carrying 18 carbon-long tails of various saturation degrees: dioleoylphosphatidylethanolamine (DOPE or 18:1 PE), 18:2 PE, 18:3 PE, dioleoylphosphatidylcholine (DOPC or 18:1 PC), 18:2 PC and 18:3 PC] and 2) the fusion efficiencies of ~150-nm ULVs (*i.e.*, large unilamellar vesicles, LUVs) as functions of C_0 and K_{cp} via tuning the lipid composition. To the best of our knowledge, the measurements are the first systematic investigation on the correlations among C_0, K_{cp}, the hydrocarbon (CH) chain saturation of a lipid and fusion. Energetic analyses on the C_0- and K_{cp}-dependences of fusion reveal the fusogenic relevance of a factor(s) other than elastic mechanics and inter-membrane interactions, whose fusogenic importance even overtakes that of C_0 and G_E, and also provide a new energetic perspective on how fusion is promoted by making C_0 more negative. The results complement the earlier studies by expanding the known effects of changing the lipid composition on the fusion energetics, and may reshape the current understanding to the fusion mechanism.

Results

Elastic properties of DOPE and DOPC. The C_0 and K_{cp} of DOPE are measured to compare against the published data to establish credibility for our experimental protocol and data. The C_0 of DOPE measured here, $C_{0,DOPE} = -0.0334 \pm 0.0001$ Å^{-1} [$=1/(-29.9 \pm 0.1)$ Å^{-1}] at 20 °C (Table 1), agrees well with the literature [*e.g.*, $C_{0,DOPE} = 1/(-30.2 \pm 0.8)$ Å^{-1} at 20 °C; $C_{0,DOPE} = 1/(-30)$ Å^{-1} at 20 °C][15,16]. The thermal variation rate of $C_{0,DOPE}$, -0.00014 ± 0.00004 Å^{-1} °C^{-1}, is also consistent with the reports by refs 15,17 (-0.00017 Å^{-1} °C^{-1} and -0.00013 ± 0.00004 Å^{-1} °C^{-1}, respectively). A similar consistency is also observed for K_{cp}, where $K_{cp,DOPE} = 0.57 \pm 0.12 \times 10^{-19}$ J ($\approx 13.9 \pm 2.9$ K_BT) at 25 °C conforms to, *e.g.*, $K_{cp,DOPE} = 0.46 \times 10^{-19}$ J (≈ 11.2 K_BT) at 20 °C in ref. 16 and $K_{cp,DOPE} = 0.53 \times 10^{-19}$ J (≈ 12.9 K_BT) at 22 °C in ref. 18.

Species		C_0 (Å^{-1})						K_{cp} (×10^{-19} J)
		15°C	20°C	25°C	30°C	35°C	40°C	25°C
DOPE		−0.0329 ± 0.0001	−0.0334 ± 0.0001	−0.0341 ± 0.0002	−0.0347 ± 0.0003	−0.035 ± 0.0002	−0.0366 ± 0.0001	0.57 ± 0.12
18:2 PE		−0.0345 ± 0.00004	−0.0350 ± 0.00005	−0.0356 ± 0.00002	−0.0361 ± 0.00005	−0.0365 ± 0.00007	−0.0379 ± 0.0002	0.33
18:3 PE		−0.0337 ± 0.00006	−0.0347 ± 0.00006	−0.0355 ± 0.00006	−0.0362 ± 0.00006	−0.0367 ± 0.00006	−0.0383 ± 0.00006	—
DOPC		−0.0094 ± 0.0005	−0.0102 ± 0.0007	−0.0106 ± 0.0008	−0.0111 ± 0.0010	−0.0116 ± 0.0009	−0.0120 ± 0.0011	—
18:2 PC		−0.0106 ± 0.0006	−0.0112 ± 0.0008	−0.0117 ± 0.0008	−0.0123 ± 0.0009	−0.0128 ± 0.0009	−0.0132 ± 0.0013	0.14
18:3 PC		−0.0086 ± 0.0007	−0.0095 ± 0.0014	−0.0099 ± 0.0015	−0.0104 ± 0.0017	−0.0109 ± 0.0019	−0.0113 ± 0.0021	0.14
DOPE/DOPC LUVs (mol% of DOPE)	0	—	—	−0.0106 ± 0.0008	—	—	—	0.40
	25	—	—	−0.0165 ± 0.0006	—	—	—	0.44
	30	—	—	−0.0177 ± 0.0006	—	—	—	0.45
	40	—	—	−0.02 ± 0.0005	—	-	—	0.47
	50	—	—	−0.0224 ± 0.0004	—	—	—	0.49
	67	—	—	−0.0264 ± 0.0003	—	—	—	0.51
Equimolar DOPE/PC LUVs (PC species)	18:1	—	—	−0.0224 ± 0.0008	—	—	—	0.49
	18:2	—	—	−0.0229	—	—	—	0.35
	18:3	—	—	−0.0220	—	—	—	0.36

Table 1. C_0 and K_{cp} of the studied lipids and LUVs.

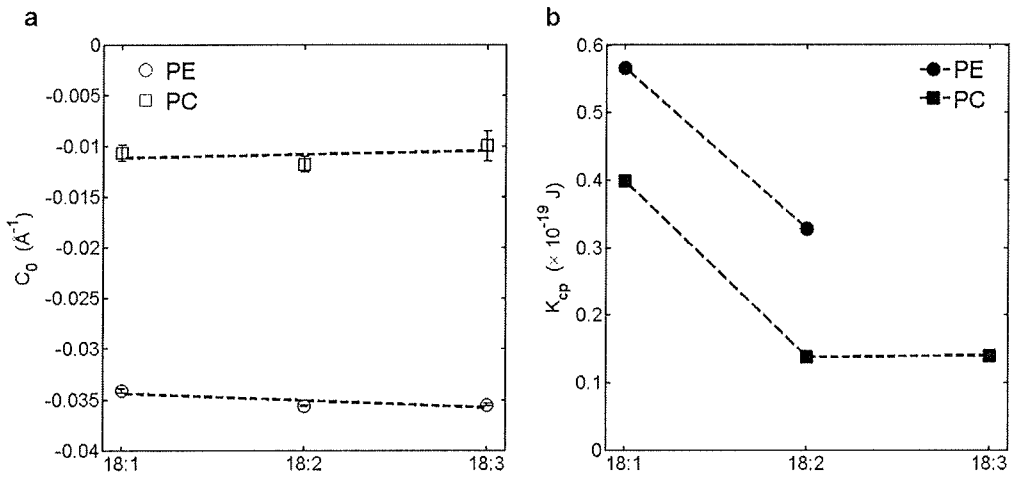

Figure 2. Dependences on the CH chain saturation of (**a**) the C_0s and (**b**) the K_{cp}s of PE and PC. Note the $K_{cp,DOPC}$ is adopted from refs 17,18.

The C_0 of DOPC, derived from the linear correlation between C_0 and lipid composition (see Methods), is measured as $C_{0,DOPC} = -0.0111 \pm 0.001$ Å^{-1} [$=1/(-90.1 \pm 8.1)$ Å^{-1}] at 30 °C and $C_{0,DOPC} = -0.0116 \pm 0.0009$ Å^{-1} [$=1/(-86.2 \pm 6.7)$ Å^{-1}] at 35 °C. These are comparable to $C_{0,DOPC} = 1/(-110.0 \pm 9.7)$ Å^{-1} at 35 °C in ref. 17 and $C_{0,DOPC} = 1/(-87.3)$ Å^{-1} at 32 °C in ref. 18. (Note that the uncertainties for $C_{0,DOPC}$s in this study and ref. 17 are intrinsic to the C_0-determination method and do not arise from experimental errors.) The thermal variation rate of $C_{0,DOPC}$, -0.00010 ± 0.00002 Å^{-1}°C^{-1}, is also agreeable with -0.00011 ± 0.00006 Å^{-1}°C^{-1} in ref. 17. The consistency with the published data validates the protocol used here and establishes credibility for the data below.

Elastic properties of the polyunsaturated PEs and PCs. The C_0 measurements for the unsaturated PEs and PCs show that carrying tails with different saturation degrees has only marginal effects on the C_0s of the lipids, with the C_0s barely shifting from $C_{0,PE} = -0.0341 \pm 0.0002$ Å^{-1} [$=1/(-29.3 \pm 0.2)$ Å^{-1}] to -0.0355 ± 0.0001 Å^{-1} [$=1/(-28.2 \pm 0.1)$ Å^{-1}] and from $C_{0,PC} = -0.0106 \pm 0.0008$ Å^{-1} [$=1/(-94.3 \pm 7.1)$ Å^{-1}] to -0.0099 ± 0.0015 Å^{-1} [$=1/(-101.0 \pm 15.3)$ Å^{-1}] when the CH chains go from monounsaturated to triunsaturated at 25 °C (Fig. 2a). This is unexpected, since CH chains with higher unsaturation degrees are more flexible and shall be more capable of assuming the splaying-out conformations, making the lipid molecules more cone-shaped and the C_0s more negative, as in raising temperature.

On the contrary, K_{cp} is dependent on the saturation degree. The K_{cp}s of PE and PC are smaller for the lipids carrying tails with higher unsaturation degrees (Fig. 2b). A monolayer is thus softer when constituted by di- or triunsaturated lipids than would be when constituted by the monounsaturated counterparts. Together with

$K_{cp,DOPC} = 0.42 \pm 0.05 \times 10^{-19}$ J at 18 °C from ref. 19 and $K_{cp,DOPC} = 0.40 \pm 0.04 \times 10^{-19}$ J at 30 °C from ref. 20, $K_{cp,PC}$ varies from $K_{cp,PC} = \sim 0.4 \times 10^{-19}$ J ($\approx$9.7 K_BT) to 0.14×10^{-19} J ($\approx$3.4 K_BT) when the number of the *cis*-double bonds in a CH chain goes from 1 to 3 (Fig. 2b). A similar trend is observed for PE: $K_{cp,PE}$ decreases from $K_{cp,PE} = 0.57 \times 10^{-19}$ J ($\approx$13.9 K_BT) to 0.33×10^{-19} J ($\approx$8 K_BT) when the chain saturation goes from monounsaturated to diunsaturated. Overall, variations by a factor of ~2 are observed for PE and PC when the CH chains go from monounsaturated to polyunsaturated.

It is noted that our results for $K_{cp,PC}$ are consistent with ref. 19: The $K_{cp,PC}$ in the reference (measured with the micropipette-aspiration technique) declined sharply from $K_{cp,PC} = 0.42 \pm 0.05 \times 10^{-19}$ J ($\approx 10.2 \pm 1.2$ K_BT) to $0.22 \pm 0.04 \times 10^{-19}$ J ($\approx 5.3 \pm 1$ K_BT) as the chains go from monounsaturated to diunsaturated, but the $K_{cp,PC}$ changed only modestly when the chains go further to triunsaturated. (Note that the property measured in ref. 19 was the *bilayer* bending modulus. Following ref. 21, this is converted to its monolayer counterpart by dividing it by 2, with the assumption of no coupling between the two monolayers). Even with different experimental techniques and an oversimplified assumption of no inter-monolayer coupling, the discrepancy between the K_{cp}s obtained here and in ref. 19 is still remarkably small. The consistency warrants the application of the experimental scheme developed here (see Methods) to measuring the K_{cp}s of the lamellar-forming lipids.

C_0 and K_{cp} dependences of fusion. Based on the C_0 and K_{cp} measurements, we manage to tune the composition of a monolayer so that one of the two properties varies while the other remains constant. This objective is achieved satisfyingly for varying K_{cp} but only with limited success for C_0. With such a composition control, we study the correlation between fusion and K_{cp} (or C_0) for LUVs. Two series of LUVs are prepared: one series composed of DOPE and DOPC with the molar fraction varied; the other composed of equimolar DOPE and PC with the PC selected from among DOPC, 18:2 PC or 18:3 PC. Fusion is initiated by PEG 8000 and detected/quantified fluorescently (fluorescence is emitted after fusion due to the complexation of the dyes, DPA and $TbCl_3$, initially encapsulated in separate LUVs; see Methods)[22].

The C_0 dependence of fusion is studied by examining fusion between the DOPE/DOPC LUVs. The *monolayer* spontaneous curvature of the LUVs, $C_{0,LUV}$, varies from -0.0106 ± 0.0008 Å^{-1} [$=1/(-94.3 \pm 7.1)$ Å^{-1})] to -0.0264 ± 0.0003 Å^{-1} [$=1/(-37.9 \pm 0.4)$ Å^{-1}], while the *monolayer* bending modulus, $K_{cp,LUV}$ (assumed to be the molar-weighted average of $K_{cp,DOPE}$ and $K_{cp,DOPC}$), is kept at a narrower range of 0.4×10^{-19} J ($\approx$9.7 K_BT) to 0.51×10^{-19} J ($\approx$12.2 K_BT), when DOPE rises from 0 mol% to 67 mol% (Table 1). As the DOPE fraction rises, the extent of fusion for the LUVs also rises (Fig. 3a). A comparison where the relative changes [relative change = 100% × {(property determined at a given [DOPE]) − (property determined at [DOPE] = 50 mol%)}/{property determined at [DOPE] = 50 mol%}] in C_0, K_{cp} and fusion are plotted against DOPE fraction demonstrates the expected correlation between fusion and $C_{0,LUV}$ reported in the literature (Fig. 3c): It was reported that ULVs with higher contents in lipids of negative C_0s, or prepared with lipids of more negative C_0s, displayed a higher propensity for fusion[13,23], while introducing to ULVs lipids of strongly positive C_0s could inhibit fusion[24], whether the systems were protein-free or contained fusogenic proteins. However, it has to be stressed that the variation in $K_{cp,LUV}$ may still be substantial enough to sway fusion, which is further discussed below.

The K_{cp} dependence of fusion is studied on the DOPE/PC LUVs. Substituting 18:2 PC or 18:3 PC for DOPC in the LUVs varies the $K_{cp,LUV}$ from 0.49×10^{-19} J ($\approx$11.8 K_BT) to 0.35×10^{-19} J ($\approx$8.6 K_BT) or 0.36×10^{-19} J ($\approx$8.6 K_BT) but retains the $C_{0,LUV}$ at ~ -0.0220 Å^{-1} [$=1/(-45.5)$ Å^{-1}] (Table 1). Surprisingly, the fluorescence intensity emitted by the dye complexes decreases drastically when the CH chains of PC go from monounsaturated to polyunsaturated; in some instances, the fluorescence for the DOPE/18:3 PC LUVs is even nearly undetectable (Fig. 3b). This sharp decline in fluorescence may originate from 1) a failure to load the dyes into the LUVs, 2) a failure to form LUVs or 3) a depression in fusion of the LUVs. The first two scenarios are excluded because (I) the fluorescence was fully recovered when the structures self-assembled by DOPE/polyunsaturated PC (whether they were LUVs or not) were disrupted by Triton X-100 (a detergent), indicating that the dyes had initially been sequestered by the self-assembled structures; and (II) the self-assembled structures were ~150 nm in size, as with the LUVs made for the rest of the study, suggesting the self-assembled structures being LUVs. Hence, we consider the reduction in fusion as the most probable cause for the sharp decline in fluorescence when the $K_{cp,LUV}$ decreases, thereby establishing a correlation between fusion and $K_{cp,LUV}$ (Fig. 3d).

Discussion

The rise in G_E of the planar monolayer, rather than the drop in G_E of stalk, is responsible for the fusion promotion induced by making C_0 more negative. The fusion promotion by making C_0 more negative has long been associated with the energetics of the fusion intermediate structures, especially hemifusion stalk[3]. Due to its hourglass shape, stalk is more energetically favorable, while a planar conformation is less favored, if the C_0s of the underlying monolayers are more negative[25]. Indeed, experiments show that using the lipid of highly negative C_0, diphytanoyl phosphatidylcholine (DPhPC), to prepare oriented bilayers allowed researchers to determine the first X-ray diffraction structure for stalk[14]; and the difference between the curvature energies [the first term in Equation (1)] of stalk and planar monolayers dropped triply when the composition of the oriented bilayers changed from DOPC alone to equimolar DOPE/DOPC, contributing to the lowering of the osmotic stress minimally needed for stabilizing stalk[6]. However, it has not been explicitly verified from experimental data whether the preference for stalk is mainly due to a rise in the elastic energy of planar monolayers or a drop in that of stalk, even though the latter is implicitly assumed to be the case in many studies. To resolve the question, we calculate the elastic energy density of a LUV, $g_{E,LUV}$, for the DOPE/DOPC LUVs via Equation (1). With the measured diameter of ~150 nm (see Methods) and the common bilayer thickness of ~4 nm for the LUVs, the Cs of the inner and outer leaflets are $-(1/740 + 1/740)$ Å^{-1} and $+(1/760 + 1/760)$ Å^{-1}, respectively, while the Gaussian curvatures ($1/740 \times 1/740$ Å^{-2} and $1/760 \times 1/760$ Å^{-2}) are negligible. (With the dimensions, the bilayer can be regarded as locally flat). Based on this and the C_0/K_{cp} data, $g_{E,LUV} = g_{E,inner\ leaflet} + g_{E,outer\ leaflet}$ is determined (Table 2).

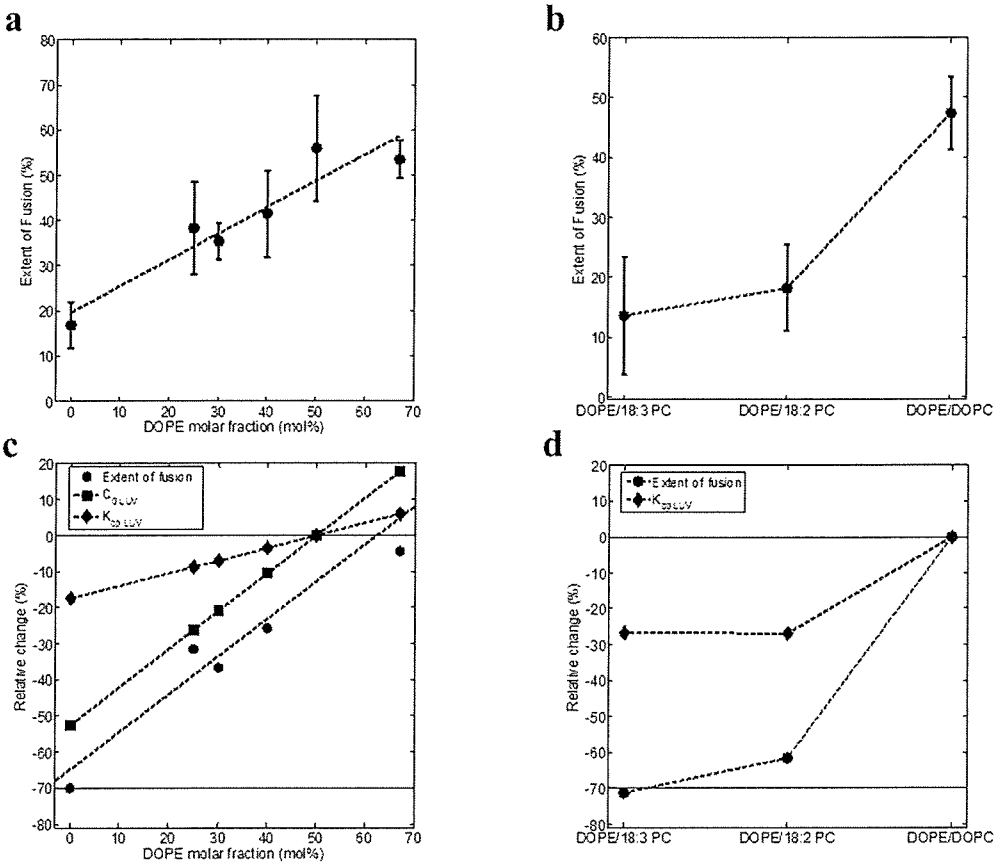

Figure 3. Fusion behavior for (**a**) the DOPE/DOPC and (**b**) the equimolar DOPE/PC LUVs. The relative changes in fusion, $C_{0,LUV}$ and $K_{cp,LUV}$ as functions of (**c**) DOPE fraction and (**d**) PC chain saturation display the correlation among fusion, C_0 and K_{cp}. The dashed lines are to guide the eyes; the solid lines in (**c**,**d**) mark the 0% and 70% changes.

Species		Elastic energy density ($\times 10^{-3}$ $K_BT/Å^2$)		
		$g_{E,inner\ leaflet}$	$g_{E,outer\ leaflet}$	$g_{E,LUV}$
DOPE/DOPC LUVs (mol% of DOPE)	**0**	0.3	0.9	1.2
	25	1.0	2.0	3.0
	30	1.2	2.3	3.5
	40	1.7	2.9	4.6
	50	2.3	3.7	6.0
	67	3.5	5.2	8.7
Equimolar DOPE/PC LUVs (PC species)	**18:1**	2.3	3.7	6.0
	18:2	1.8	2.8	4.6
	18:3	1.6	2.6	4.2

Table 2. Calculated elastic energy densities of the LUVs.

The $g_{E,LUV}$ steadily rises along with the DOPE fraction, leading to its positive correlation with fusion (the Pearson correlation coefficient is 0.8889, Fig. 4), *i.e.*, the higher the $g_{E,LUV}$ is, the more the LUVs are inclined to fusing. The variation in C_0 alone accounts for >75% of the change in $g_{E,LUV}$. Thus, the result establishes a correlation among C_0, $g_{E,LUV}$ and fusion: Making C_0 more negative elevates $g_{E,LUV}$, which in turn promotes fusion. More specifically, making C_0 more negative aggravates the energetic penalty of keeping the monolayers in the planar conformation, causing the transformation to stalk more appealing in comparison.

The remaining question is: Does making C_0 more negative also reduce the elastic energy of stalk? We deduce the elastic energies (defined against the reference point, the elastic energy of a monolayer with $C_0 = 0$ and in the planar conformation), G_Es, of the *cis*-monolayers in the planar and stalk conformations. The difference, $\Delta G_{E,ps}$, between G_Es of the two conformations can be expressed as[6],

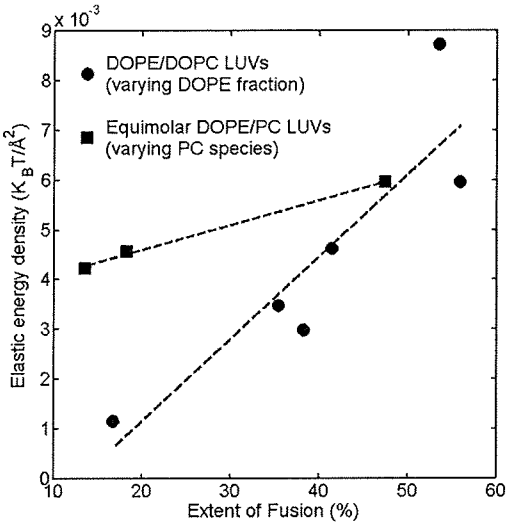

Figure 4. $g_{E,LUV}$ versus fusion for the DOPE/DOPC LUVs with the DOPE fraction varied, and for the equimolar DOPE/PC LUVs with the PC species changed. The dashed lines are to guide the eyes.

$$\Delta G_{E,ps} = G_{E,stalk} - G_{E,planar} = \left[\frac{1}{2}K_{cp}\int_A (C - C_0)^2 dA + K_G\int_A GdA\right] - \left[\frac{1}{2}K_{cp}\int_A C_0^2 dA\right] = K_{cp}(\Sigma_1 + C_0\Sigma_2) - 4\pi K_G, \quad (2)$$

with

$$\Sigma_1 = \int_A \frac{C^2}{2} dA = \frac{A}{2}\langle C^2\rangle_A, \quad \Sigma_2 = -\int_A CdA = -A\langle C\rangle_A,$$

$\langle\ldots\rangle_A$ is the average over surface area A) and,

$$K_G\int_A GdA = -4\pi K_G,$$

for stalk. Based on our $C_0/K_{cp}/g_{E,LUV}$ data, $(\Sigma_1, \Sigma_2) = (7.84, 207.6)$ for DOPC alone and $(\Sigma_1, \Sigma_2) = (6.81, 200.5)$ for equimolar DOPE/DOPC[6] and $K_G \approx 8$ K_BT[26], $\Delta G_{E,ps}$ is determined to be ~155 K_BT and ~128 K_BT for the *cis*-monolayers made of DOPC alone and equimolar DOPE/DOPC, respectively. The shrink in the $\Delta G_{E,ps}$ upon introducing DOPE is consistent with what is seen for $g_{E,LUV}$. By adopting from ref. 6 the surface areas of ~7,600 Å^2 for monolayers made of DOPC alone and ~8,700 Å^2 for equimolar DOPE/DOPC, G_E of the *cis*-monolayers in the planar conformation is determined as $G_{E,planar} = g_{E,outer\ leaflet} \times 7{,}600 = 6.5$ K_BT (or 0.27×10^{-19} J) for DOPC alone and 32.0 K_BT (or 1.32×10^{-19} J) for equimolar DOPE/DOPC. Again, the result is consistent with the observation for $g_{E,LUV}$. We deduce G_E of stalk by summing the corresponding $\Delta G_{E,ps}$ and $G_{E,planar}$. Strikingly, the deduced $G_{E,stalk}$ is ~160 K_BT for the *cis*-monolayers made of both DOPC alone and equimolar DOPE/DOPC. In contrast, $G_{E,planar}$ differs by a factor of 5 or ~26 K_BT upon the same change in the composition.

The invariability of $G_{E,stalk}$ may suggest that $G_{E,stalk}$ is a conserved property for monolayers and irrespective of the composition, at least for the two compositions considered here. Given the intimacy between G_E and the overall geometry of a structure, this may further imply that the overall geometry of stalk is also universal among monolayers of various compositions. Indeed, experimental and computational studies have shown that the overall geometry of stalk is highly conserved among monolayers of diverse compositions[6], as well as among various coarse-grained models used in the computational studies[9]. Given the energetic/geometric invariability of stalk and the variation in $G_{E,planar}$ upon changing C_0, we argue that the fusion promotion by making C_0 more negative is effected mainly via a rise in $G_{E,planar}$, rather than a drop in $G_{E,stalk}$.

Some may wonder: Equation (1) demands $g_{E,stalk}$ to vary with C_0 if C is constant (as seemingly entailed by the geometric invariability of stalk). Thus, how can $G_{E,stalk}$ remains unchanged when the composition varies? One has to realize that the conservation in geometry is *not* equivalent of the conservation in *dimension*, or more specifically, in C. C of stalk may vary with the composition so that $G_{E,stalk}$ is unchanged. Indeed, the X-ray diffraction structures of stalk indicate that $\langle C\rangle_A$ of stalk is ~1/36.6 Å^{-1} for DOPC alone and ~1/43.4 Å^{-1} for equimolar DOPE/DOPC[6].

Changes in the inter-membrane interactions and in G_Es of stalk, HD and FP cannot account for the fusion reduction upon raising the chain unsaturation. Several factors may account for the apparent $K_{cp,LUV}$-fusion correlation (Fig. 3d). Among these factors is the modulation of the inter-membrane repulsion arising from the membrane undulational motion (*i.e.*, the out-of-plane fluctuation of membrane); enhancing the repulsion would prevent the LUVs from shortening the inter-membrane distances and thus stymie the fusion initiation. The undulation repulsion is entropic in nature, and proportional to temperature while inversely proportional to K_{cp}[27]; the inverse proportionality to K_{cp} is consistent with the observed $K_{cp,LUV}$-fusion correlation. To explore the fusogenic relevance of the undulation repulsion, we examine the sizes of the equimolar DOPE/PC LUVs before and after the addition of PEG 8000 with dynamic light scattering. Interestingly, while the DOPE/DOPC LUVs increase their diameters from ~150 nm to ~600 nm, as expected for fusion, the diameter of DOPE/18:2 PC LUVs also expands considerably from ~150 nm to >600 nm (Supplementary Fig. S5). Together with the result of the content-mixing fusion assays for the latter LUV species (Fig. 3b), we infer that raising the chain unsaturation does not prevent the LUVs from approaching one another but still considerably compromises their capabilities of completing the fusion process. Therefore, enhancement of the inter-membrane repulsions is not expected to be responsible for the correlation between chain saturation and fusion.

The apparent $K_{cp,LUV}$-fusion correlation may alternatively arise from the influence on G_E of varying K_{cp}. We again deduce $G_{E,planar}$ and $\Delta G_{E,ps}$ to explore the underlying mechanism in the context of stalk formation. The surface area of the *cis*-monolayers is assumed to remain ~8,700 Å^2, even though the PC of the equimolar DOPE/PC monolayers is either 18:2 PC or 18:3 PC rather than DOPC (the interfacial areas of lipids with the same headgroup but distinct chains differ marginally when they are in the same phase at a given temperature)[28,29]. The deduced $G_{E,planar}$s are 32.0 K_BT, 24.4 K_BT and 22.8 K_BT for DOPE/DOPC, DOPE/18:2 PC and DOPE/18:3 PC, respectively. The variation is modest in comparison with the case where the DOPE fraction (and C_0) of the DOPE/DOPC monolayers is varied. On the other hand, we expect the energetic/geometric invariability of stalk to be valid for the DOPE/PC monolayers and $G_{E,stalk}$ to remain ~160 K_BT, because the stalk geometry is highly conserved among monolayers made of a wide variety of lipids (including DPhPC, which carries bulky CH chains)[6]. Hence, $\Delta G_{E,ps}$ is ~136.5 K_BT for both DOPE/18:2 PC and DOPE/18:3 PC. Thus, varying K_{cp} by ~27%, while steadying C_0 at ~−0.0220 Å^{-1}, only raises $\Delta G_{E,ps}$ from ~128 K_BT to ~136.5 K_BT. Interestingly, this modest rise by ~8.5 K_BT is sufficient to reduce fusion by 70% (Fig. 3d), while the same extent of decline in fusion is reached only when $\Delta G_{E,ps}$ increases by ~27 K_BT for the case of varying the DOPE fraction (Fig. 3c). The large discrepancy between the two cases indicates that an extra factor(s), other than the elastic energy involved in the planar-to-stalk transformation, may act to dictate fusion. Indeed, as shown in Fig. 4, the variation in fusion is less correlated with $g_{E,LUV}$ for varying the PC species than for varying the DOPE fraction.

In addition to the one related to stalk, G_Es of HD and FP may also contribute to the apparent $K_{cp,LUV}$-fusion correlation. To examine the significance of these contributions, we numerically estimate how the G_Es would vary with $K_{cp,LUV}$ upon substituting 18:2 PC for DOPC through,

$$G_E = \frac{1}{2}K_{cp}\int_A (C - C_0)^2 dA + K_G\int_A GdA = \frac{1}{2}K_{cp}A\langle (C - C_0)^2\rangle_A - 4\pi K_G. \quad (3)$$

K_Gs of the LUVs are estimated by multiplying their K_{cp}s with the ratio of $-K_G/K_{cp}$, which is about 0.84 for DOPC, DOPE and even their mixtures with other lipids (e.g., DOPC/sphingomyelin/cholesterol)[30]. Integrating G over a given surface area also yields -4π for both HD and FP due to the identity of their topological genus to that of stalk[31]. Due to the lack of information on how Cs of HD and FP vary locally and with the composition, we adopt a wide range of Cs, $-0.05 \le C \le +0.018$, for our estimation to include all possible variations in C, with the lower limit more negative than any known negative C_0 for a phospholipid[17] and the upper limit even greater than Cs of the most curved region of FP[32]. The result shows that $G_{E,HD}$ and $G_{E,FP}$ would be constantly higher for DOPE/DOPC than for DOPE/18:2 PC, however C varies locally and with the composition (Table 3). This result contradicts with the observation that the DOPE/DOPC LUVs fuse more readily than the DOPE/18:2 PC LUVs (Fig. 3b), thus suggesting the irrelevance of $G_{E,HD}$ and $G_{E,FP}$ to the observed difference in fusion.

Conclusion

Overall, neither the modulation of inter-membrane interactions nor the changes in $\Delta G_{E,ps}$, $G_{E,stalk}$, $G_{E,HD}$ and $G_{E,FP}$ ($G_{E,HD}$ and $G_{E,FP}$ decrease even when fusion is suppressed!) can account for the apparent $K_{cp,LUV}$-fusion correlation. This may indicate the presence of an unrecognized factor that is subject to K_{cp} and dictates fusion. It is known from Fig. 3c,d that fusion is depressed by ~70% when one either decreases K_{cp} by ~17% *plus* C_0 by >50%, or simply decreases K_{cp} by ~27% without varying C_0. It seems that depressing K_{cp} to enhance this unrecognized factor alone is sufficient to suppress fusion to a great extent; if K_{cp} is slightly less depressed, the same extent of fusion suppression is achieved only when C_0 is simultaneously changed by a much larger degree. It is thus tempting to claim that this factor is at least as important as C_0 and G_E in dictating fusion, if not more so. Another possibility is that the variation in K_{cp} is only a consequence of changing the LUV composition and does not directly affects fusion; it is another effect arising from the composition change that is responsible for the differential fusion capabilities. One such candidate is the variation in the tilt modulus, which is associated with the CH chain stretching and tilting when the chains are arranged to form stalk and HD[33,34]. Indeed, raising the chain unsaturation increases the tilt modulus[35,36] and may thus aggravate the related energetic penalties of maintaining stalk and HD[34]. Another candidate is the variation in the hydrophobic interactions arising from exposing the CH chains of *cis*-monolayers to water during the stalk formation[34]. Nevertheless, quantifying the contributions of the two effects is out of the scope of the paper. Further studies are still desired to quantify the effects or to identify other responsible factor(s).

Lipid composition		Curvature energy term				Gaussian term			G_E
		K_{cp} ($\times 10^{-19}$ J)	C (Å)	C_0 (Å)	$K_{cp}A(C-C_0)^2/2$ ($\times 10^{-19}$ J)	K_G	$\int GdA$	$K_G\int GdA$ ($\times 10^{-19}$ J)	($\times 10^{-19}$ J)
DOPE/DOPC	Negative C	0.49	−0.05 ~ −0.022	−0.022	1.67 ~ 0	−0.41	-4π	5.15	6.82 ~ 5.15
			−0.022 ~ 0		0 ~ 1.03				5.15 ~ 6.18
	Positive C		0 ~ 0.018		1.03 ~ 3.41				6.18 ~ 8.56
DOPE/18:2PC	Negative C	0.35	−0.05 ~ −0.022	−0.022	1.19 ~ 0	−0.29	-4π	3.64	4.84 ~ 3.64
			−0.022 ~ 0		0 ~ 0.74				3.64 ~ 4.38
	Positive C		0 ~ 0.018		0.74 ~ 2.44				4.38 ~ 6.08

Table 3. Elastic energy estimations for the monolayers of HD and FP in different compositions.

Conventionally, upon introducing to membranes lipids of highly negative or positive C_0s, the change in fusion is often attributed to the change in C_0 (and consequently in G_E), while the accompanying variations in K_{cp} and/or other potential factors are overlooked. By examining the apparent $K_{cp,LUV}$-fusion correlation, we have demonstrated that a factor(s) other than the variations in C_0 and G_E, which is affected by or accompanies the K_{cp} variation, plays a key role in dictating fusion when the membrane composition is changed; the fusogenic importance of the factor(s) may even overtake the importance of C_0 or membrane elastic energetics in general. We therefore suggest that caution shall be used when one interprets the influence on fusion of varying C_0 via membrane composition changes. This understanding, along with the conclusion that promoting fusion by making C_0 more negative is effected via a rise in $G_{E,planar}$, may reshape the energetic considerations on fusion, particularly the roles of fusogenic proteins in regulating cellular fusion machineries.

This study also made two intriguing observations: (1) Modulating the chain saturation (with the length fixed) of a lipid from monounsaturated to triunsaturated has virtually no effect on its C_0. The observation falsifies the expectation that raising the unsaturation degree always makes C_0 more negative; (2) our developed scheme enables the application of the osmotic stress method to the K_{cp} measurements for lipids not preferring the formation of the hexagonal H_{II} phase (formation of the phase is a prerequisite for the conventional osmotic stress method), providing an extra means for the K_{cp} determination.

Methods

C_0 Measurement. Excessive buffer containing 10 mM HEPES with pH ≈ 7.4 was used to suspend a dried mixture of lipid and tetradecane. The dispersion was shuffled between two glass syringes for >100 runs and underwent >10 freeze-thaw cycles for homogenization. Each sample had *a* fixed lipid composition and contained 16 wt% tetradecane. The measurements by X-ray diffraction were carried out with Cu $K\alpha$ or synchrotron radiation (BL13A1 and BL23A1 of NSRRC, Hsinchu, Taiwan). The diffraction images were recorded with a Pilatus 100 K pixel (Dectris, Switzerland), a Mar165 CCD and a Pilatus 1MF pixel detectors for Cu $K\alpha$, BL13A and BL23A1, respectively.

Data were collected at 15 °C to 40 °C with a 5 °C interval. The reduced, azimuthally integrated and background-subtracted 1-D diffraction profiles of the lipids forming the H_{II} phase were used to reconstruct the electron density profiles through $\rho_e(\vec{r}) = \rho_{avg} + \sum_q A_q \cos(\vec{q}\cdot\vec{r})$ and $A_q^2 \propto \frac{I_q \sin\theta}{m}$, where I_q is the diffraction intensity, $\sin\theta$ the Lorentz correction and m the multiplicity factor[37]. Following the method in ref. 15, the radial distances, R_ps, between the H_{II} center and the pivotal plane were extracted from the profiles and experimentally determined the C_0s of the H_{II}-forming PEs. For the PCs, which preferred the formation of lamellar phases, a series of binary DOPE/PC mixtures were prepared; the molar fractions were controlled such that H_{II} was the sole stable phase in excess water and tetradecane and the mixture C_0s were determined as for DOPE alone. The C_0s showed linear correlations with the PC fraction (Supplementary Fig. S1). Extrapolating the correlations to pure PC yielded its C_0. A sample, with a fixed lipid composition, only contributed to a data point in Supplementary Fig. S1.

K_{cp} Measurement. Except that the buffer contained PEG 8000 and the data were taken at 25 °C only, the samples were prepared similarly as above. Given the Flory radius of ~8 nm, PEG molecules could not enter the H_{II} water core (<4 nm) and thus applied an osmotic stress on H_{II}. The consequent structural deformation of H_{II} was given by $\Pi R_p^2 = 2K_{cp}\left(\frac{1}{R_p} - \frac{1}{R_{0p}}\right)$, where Π is the osmotic stress and $R_{op} = 1/C_0$[16]. The slopes of the ΠR_p^2-versus-$1/R_p$ relation gave the K_{cp}s of the H_{II}-forming PEs. An experimental scheme was developed to measure the K_{cp}s of the lamellar-forming PCs. A series of binary DOPE/PC mixtures were prepared and individually subjected to various osmotic stresses when H_{II} was the sole stable phase in excessive buffer and tetradecane. Supplementary Fig. S2 exemplifies the data thereby collected. Based on such data, we obtained the ΠR_p^2-versus-$1/R_p$ relations for DOPE/18:3 PC and DOPE/18:2 PC of various molar ratios (Supplementary Fig. S2b) and extracted the K_{cp}s of the mixtures. (Note *each* data point in supplementary Fig. S2 corresponds to *an* independently prepared sample.) We then established the K_{cp}-composition relations for the mixtures, which were mostly linear (Supplementary Fig. S3) and could determine the K_{cp}s of the PCs as pure substances. 16 independent samples were in average used to determine the K_{cp} of a PC, which is thus statistically sound and representative.

Fusion Assay. Two populations of ULVs encapsulating either $TbCl_3$ or DPA (fluorescent dyes) were prepared with extrusion[38]. A dried mixture of DOPE, PC and DOPA was prepared similarly as above, with the DOPA fixed at 4 mol% and *no* tetradecane added. (Adding DOPA was to introduce negative surface charges to facilitate the ULV formation; owing to the tiny, fixed amount and $C_{0,DOPA} \approx C_{0,DOPC}$ the DOPA contribution was negligible[15,39]).

Buffer containing either (a) 2.5 mM $TbCl_3$, 50 mM sodium citrate and 10 mM HEPES (pH = 7.4) or (b) 50 mM DPA and 10 mM HEPES (pH = 7.4) was used to suspend the lipid mixtures and the final lipid concentration was 5 mg/ml. Extrusion was carried out with Mini-Extruder system (Avanti) and a polycarbonate membrane at 40 °C. Unloaded dyes were removed with dialysis (3.5K MWCO, SnakeSkin dialysis tubing). The lipid concentrations were unchanged throughout the dialysis. Removal of unloaded dyes was confirmed by the lack of fluorescence from mixing the two ULV populations in the absence of PEG 8000. Small-angle X-ray scattering confirmed the ULV formation, rather than MLVs (Supplementary Fig. S4). The ULV size was measured with dynamic light scattering at 25 °C. Regardless of the composition, *all* our ULV samples had the average diameter of ~150 nm with narrow size distributions (Supplementary Fig. S5, upper panels).

Fusion was quantified with fluorescence from the DPA/$TbCl_3$ complexes formed upon fusion of the LUVs. The assay was carried out by mixing the solutions of (a) DPA-loading LUVs, (b) $TbCl_3$-loading LUVs, and (c) 50 wt% PEG 8000 and 1 mM EDTA, in the ratio of 100:100:800 μl. PEG 8000 initiated fusion by modifying the water chemical potential and hydration repulsion. The emission at 545 nm upon fusion was excited at 276 nm in a spectrofluorometer at 25 °C. The extent of fusion was determined as: Extent of fusion (%) $= \frac{I_{sample} - I_0}{I_{Max} - I_0} \times 100\%$, where I_{sample} and I_0 were the intensities of the sample at equilibrium and before fusion, respectively; and I_{Max} was the maximally possible intensity and obtained by adding 0.1% (v/v) Triton X-100, which disrupted the LUVs and released the dyes to maximize the number of the complexes formed. In measuring I_{sample}, EDTA was present outside the LUVs to sequester leaked $TbCl_3$ so that the detected emission was from fusion.

References

1. Jahn, R. & Fasshauer, D. Molecular machines governing exocytosis of synaptic vesicles. *Nature* **490,** 201–207 (2012).
2. Connolly, S. A., Jackson, J. O., Jardetzky, T. S. & Longnecker, R. L. Fusing structure and function: a structural view of the herpesvirus entry machinery. *Nat. Rev. Microbiol.* **9,** 369–381 (2011).
3. Chernomordik, L. V. & Kozlov, M. M. Mechanics of membrane fusion. *Nat. Struct. Mol. Biol.* **15,** 675–683 (2008).
4. Wickner, W. & Schekman, R. Membrane fusion. *Nat. Struct. Mol. Biol.* **15,** 658–664 (2008).
5. Marsden, H. R., Tomatsu, I. & Kros, A. Model systems for membrane fusion. *Chem. Soc. Rev.* **40,** 1572–1585 (2011).
6. Aeffner, S., Reusch, T., Weinhausen, B. & Salditt, T. Energetics of stalk intermediates in membrane fusion are controlled by lipid composition. *Proc. Natl. Acad. Sci. USA* **109,** E1609–E1618 (2012).
7. Khattari, Z., Köhler, S., Xu, Y., Aeffner, S. & Salditt, T. Stalk formation as a function of lipid composition studied by X-ray reflectivity. *Biochim. Biophys. Acta* **1848,** 41–50 (2015).
8. Rand, R. P. & Parsegian, V. A. Hydration forces between phospholipid bilayers. *Biochim. Biophys. Acta* **988,** 351–376 (1989).
9. Fuhrmans, M., Marelli, G., Smirnova, Y. G. & Müller, M. Mechanics of membrane fusion/pore formation. *Chem. Phys. Lipids* **185,** 109–128 (2015).
10. Siegel, D. P. & Epand, R. M. The mechanism of lamellar-to-inverted hexagonal phase transitions in phosphatidylethanolamine: implications for membrane fusion mechanisms. *Biophys. J.* **73,** 3089–3111 (1997).
11. Seddon, J. M. Structure of the inverted hexagonal (H_{II}) phase, and non-lamellar phase transitions of lipids. *Biochim. Biophys. Acta* **1031,** 1–69 (1990).
12. Gruner, S. M. Stability of lyotropic phases with curved interfaces. *J. Phys. Chem.* **93,** 7562–7570 (1989).
13. Churchward, M. A. *et al.* Specific lipids supply critical negative spontaneous curvature—an essential component of native Ca^{2+}-triggered membrane fusion. *Biophys. J.* **94,** 3976–3986 (2008).
14. Yang, L. & Huang, H. W. Observation of a membrane fusion intermediate structure. *Science* **297,** 1877–1879 (2002).
15. Chen, Y. F., Tsang, K. Y., Chang, W. F. & Fan, Z. A. Differential dependencies on [Ca2+] and temperature of the monolayer spontaneous curvatures of DOPE, DOPA and cardiolipin: effects of modulating the strength of the inter-headgroup repulsion. *Soft Matter.* **11,** 4041–4053 (2015).
16. Fuller, N., Benatti, C. R. & Rand, R. P. Curvature and bending constants for phosphatidylserine-containing membranes. *Biophys. J.* **85,** 1667–1674 (2003).
17. Kollmitzer, B., Heftberger, P., Rappolt, M. & Pabst, G. Monolayer spontaneous curvature of raft-forming membrane lipids. *Soft Matter.* **9,** 10877–10884 (2013).
18. Chen, Z. & Rand, R. P. The influence of cholesterol on phospholipid membrane curvature and bending elasticity. *Biophys. J.* **73,** 267–276 (1997).
19. Rawicz, W., Olbrich, K. C., McIntosh, T., Needham, D. & Evans, E. Effect of chain length and unsaturation on elasticity of lipid bilayers. *Biophys. J.* **79,** 328–339 (2000).
20. Liu, Y. & Nagle, J. F. Diffuse scattering provides material parameters and electron density profiles of biomembranes. *Phys. Rev. E* **69,** 040901 (2004).
21. Marsh, D. Elastic curvature constants of lipid monolayers and bilayers. *Chem. Phys. Lipids* **144,** 146–159 (2006).
22. Käsbauera, M., Lasicb, D. D. & Winterhalterc, M. Polymer induced fusion and leakage of small unilamellar phospholipid vesicles: effect of surface grafted polyethylene-glycol in the presence of free PEG. *Chem. Phys. Lipid* **86,** 153–159 (1997).
23. Chang, J. *et al.* Fusion step-specific influence of cholesterol on SNARE-mediated membrane fusion. *Biophys. J.* **96,** 1839–1846 (2009).
24. Churchward, M. A., Rogasevskaia, T., Höfgen, J., Bau, J. & Coorssen, J. R. Cholesterol facilitates the native mechanism of Ca2+ -triggered membrane fusion. *J. Cell Sci.* **118,** 4833–4848 (2005).
25. Katsov, K., Müller, M. & Schick, M. Field theoretic study of bilayer membrane fusion. I. Hemifusion mechanism. *Biophys. J.* **87,** 3277–3290 (2004).
26. Siegel, D. P. The Gaussian curvature elastic energy of intermediates in membrane fusion. *Biophys. J.* **95,** 5200–5215 (2008).
27. Leckband, D. & Israelachvili, J. Intermolecular forces in biology. *Q. Rev. Biophys.* **34,** 105–267 (2001).
28. Kucerka, N., Tristram-Nagle, S. & Nagle, J. F. Structure of fully hydrated fluid phase lipid bilayers with monounsaturated chains. *J. Membr. Biol.* **208,** 193–202 (2005).
29. Kucerka, N. *et al.* Structure of fully hydrated fluid phase DMPC and DLPC lipid bilayers using X-ray scattering from oriented multilamellar arrays and from unilamellar vesicles. *Biophys. J.* **88,** 2626–2637 (2005).
30. Hu, M., Briguglio, J. J. & Deserno, M. Determining the Gaussian curvature modulus of lipid membranes in simulations. *Biophys. J.* **102,** 1403–1410 (2012).
31. Siegel, D. P. & Kozlov, M. M. The gaussian curvature elastic modulus of N-monomethylated dioleoylphosphatidylethanolamine: relevance to membrane fusion and lipid phase behavior. *Biophys. J.* **87,** 366–374 (2004).
32. Jackson, M. B. Minimum membrane bending energies of fusion pores. *J. Membr. Biol.* **231,** 101–115 (2009).
33. Kozlovsky, Y. & Kozlov, M. M. Stalk model of membrane fusion: solution of energy crisis. *Biophys. J.* **82,** 882–895 (2002).

34. Ryham, R. J., Klotz, T. S., Yao, L. & Cohen, F. S. Calculating Transition Energy Barriers and Characterizing Activation States for Steps of Fusion. *Biophys. J.* **110,** 1110–1124 (2016).
35. Jablin, M. S., Akabori, K. & Nagle, J. F. Experimental support for tilt-dependent theory of biomembrane mechanics. *Phys. Rev. Lett.* **113,** 248102 (2014).
36. Jablin, M. S., Akabori, K. & Nagle, J. F. Experimental Assessment of Tilt-Dependent Thermal Fluctuations in Lipid Bilayers. *Biophys. J.* **108** (suppl. 1), p84a (2015).
37. Harper, P. E., Mannock, D. A., Lewis, R. N., McElhaney, R. N. & Gruner, S. M. X-ray diffraction structures of some phosphatidylethanolamine lamellar and inverted hexagonal phases. *Biophys. J.* **81,** 2693–2706 (2001).
38. Lapinski, M. M., Castro-Forero, A., Greiner, A. J., Ofoli, R. Y. & Blanchard, G. J. Comparison of liposomes formed by sonication and extrusion: rotational and translational diffusion of an embedded chromophore. *Langmuir* **23,** 11677–11683 (2007).
39. Israelachvili, J. & Wennerström, H. Entropic forces between amphiphilic surfaces in liquids. *J. Phys. Chem.* **96,** 520–531 (1992).

Acknowledgements

This study is supported by the Ministry of Science and Technology (Grant no.: MOST 104-2221-E-008-113-MY2) and by National Central University. We thank the scientific and technical supports from the staff scientists of Beamlines BL13A and BL23A of NSRRC.

Author Contributions

Z.-A.F. and K.-Y.T. contributed equally to the work. Y.-F.C. initiated and laid out the strategy for the work. Z.-A.F., K.-Y.T. and Y.-F.C. designed the experiments. Z.-A.F., K.-Y.T. and S.-H.C. performed the experiments. Z.-A.F., K.-Y.T. and Y.-F.C. processed, analyzed and drew conclusions from the data. Y.-F.C. supervised the work and wrote the paper. All authors reviewed the manuscript.

Additional Information

Supplementary information accompanies this paper at http://www.nature.com/srep

Competing financial interests: The authors declare no competing financial interests.

How to cite this article: Fan, Z.-A. *et al.* Revisit the Correlation between the Elastic Mechanics and Fusion of Lipid Membranes. *Sci. Rep.* **6,** 31470; doi: 10.1038/srep31470 (2016).

This work is licensed under a Creative Commons Attribution 4.0 International License. The images or other third party material in this article are included in the article's Creative Commons license, unless indicated otherwise in the credit line; if the material is not included under the Creative Commons license, users will need to obtain permission from the license holder to reproduce the material. To view a copy of this license, visit http://creativecommons.org/licenses/by/4.0/

© The Author(s) 2016